Control and Efficiency Analysis for a Lundell-Alternator/Active-Rectifier System in Automotive Applications

Dimitrios Sarafianos, Danilo X. Llano,
Bo Wen and Timothy J. Flack
Department of Engineering
University of Cambridge
United Kingdom, Cambridge CB3 0FA
Email:d.n.sarafianos@gmail.com

Richard A. McMahon
WMG
University of Warwick
United Kingdom, Coventry CV4 7AL

Stephen Pickering
JaguarLandRover Ltd.
United Kingdom, Coventry

***Abstract*—This paper presents a control strategy for a conventional Lundell alternator and an active-rectifier. The control scheme focuses on the minimisation of the stator copper losses of the alternator in an effort to maximise its efficiency. The modulation scheme of the active-rectifier is being investigated with the introduction of three different modulation techniques in order to quantify the effect they have on the alternator's efficiency. Steady-state results from experimental measurements of the alternator rectifier system are compared against a standard passive rectifier. The comparison indicates that the modulation scheme of the active-rectifier is significant to the alternator's efficiency as well as to the overall system efficiency.**

***Index Terms*—Active-rectifier, Lundell machine**

I. Introduction

THE Lundell alternator is the predominant machine used as a generator in conventional vehicles due to its robustness, wide speed range and cost [1]. Research has been focused on mitigating the inevitable inefficiencies of the existing power generation system either by maximising the power capability of the alternator or improving the efficiency of the rectification stage.

Rees and Ammann [2] propose a synchronous rectification scheme, resulting in efficiency improvement at the low speed end of the alternator. In [3] a MOSFET bridge using synchronous rectification is analysed quantifying the efficiency improvement via fuel consumption. Gorman et al. [4] introduce a synchronous rectifier to maximise the alternator's power at idle speed. In [5] the authors propose a cost-effective method for introducing a MOSFET synchronous rectifier and a control scheme to maximise the output power of the alternator. Efficiency improvement is achieved at idle speed and the work is extended in [6] for the whole speed range of the alternator by introducing winding reconfiguration at 3000 rpm achieving efficiency improvement at cruising speed. In [7] the authors propose power maximisation of a Lundell alternator using either winding reconfiguration or a number of different rectifier topologies. An IGBT based active-rectifier with sine-triangle Pulse Width Modulation (sPWM) is presented [7]. It is concluded that at the low speed end the efficiency of the alternator is increased but not for idle speed, which is decreased [7]. At high speed operation, greater than 4000 rpm, the anti-parallel diodes of the IGBTs are used as a passive rectifier because the sPWM rectifier cannot deliver more power at that speed range [7]. However, the use of IGBTs instead of MOSFETs increases the voltage drop of the rectifier, while the control scheme used is not analysed.

This paper examines the active-rectifier control scheme challenges imposed by the high stator inductance of the Lundell alternator and the low dc-link voltage (14 V). The aim of this paper is to investigate the efficiency improvement of the automotive electrical power generation system, by introducing an active-rectifier using MOSFETs and a control strategy based on a cost function that minimises copper losses. The proposed solution is implemented using three different modulation schemes; sPWM; sPWM with injection of 1/6th of the third harmonic component; Discontinuous Space Vector Modulation (DSVM) to examine the effects of the PWM modulation strategies in the rectifier and system efficiency.

The paper is organised as follows; first, the mathematical model of the generator is presented. Later on, the strategy to calculate the current reference values is developed in an effort to reduce the stator copper losses of the alternator and evaluate the operation of the system. Then, the control strategy is implemented in a Matlab/Simulink alternator model coupled to an active-rectifier, in order to design the cascaded PI controllers scheme. Different modulation schemes are analysed. Finally, an alternator test-rig is used to to generate and compare steady-state experimental efficiency results from the operation of the active and passive rectifier.

II. Model of the System

A Bosch LiX 180 A three-phase sixteen-pole delta-connected alternator is used as the generator. The field is aligned to the d-axis thus the generated back-emf voltage is

This work was financially supported by JaguarLandRover Ltd.

978-1-5090-1546-7/16/$31.00 ©2016 IEEE

aligned to the q-axis. Therefore, rotor position sensing allows to achieve field oriented control [8].

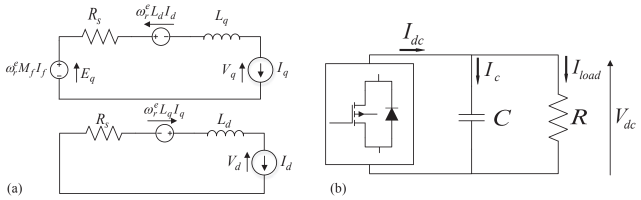

Fig. 1. a) Stator circuit of the Lundell alternator b) DC side of the active-rectifier [8].

The mathematical representation of the stator voltages at the dq rotor reference frame, seen in Fig.1.a, is given by equations (1) and (2) and of the rotor field winding circuit by equation (3) [9].

$$0 = V_d + R_s I_d + L_d p I_d - \omega_r^e L_q I_q \tag{1}$$

$$\omega_r^e M_f I_f = V_q + R_s I_q + L_q p I_q + \omega_r^e L_d I_d \tag{2}$$

$$V_f + M_f p I_d = (R_f + p L_f) I_f \tag{3}$$

where V_{dq} are the dq stator voltages, V_f is the field winding voltage, I_{dq} are the dq stator currents, I_f is the rotor field current, R_s is the stator resistance, R_f is the rotor resistance, M_f is the mutual inductance between the stator and the rotor, L_d is the d-axis stator inductance, L_q is the q-axis stator inductance, L_f is the rotor inductance. ω_r^e is the electrical speed and 'p' is the time-differential operator.

The active-rectifier is modelled considering the power balance between the ac and the dc side ($P_{ac} = P_{dc}$) of the rectifier and ignoring its losses:

$$\frac{3}{2}(V_q I_q + V_d I_d) = V_{dc} I_{dc} \Rightarrow I_{dc} = \frac{3}{2}(m_q I_q + m_d I_d) \tag{4}$$

m_d and m_q are the modulation indexes of the rectifier in the d-axis and q-axis respectively. The dc current (I_{dc}) of the rectifier, as seen in Fig.1.b, is equal to:

$$I_{dc} = I_c + I_{load} = C\frac{dV_{dc}}{dt} + \frac{V_{dc}}{R} \tag{5}$$

These equations are coupled together to describe the investigated system and assist at the development of the control strategy.

III. Control challenges

The active rectification of a Lundell alternator at 14V dc-link bus sets a number of constraints. First, Lundell alternators feature a high stator inductance [10]. Considering that a typical alternator speed range spans between 2000 rpm and 15000-18000 rpm and the pole-pair number varies between 6 to 8 [1], it becomes evident that the synchronous reactance will be high, especially at high speed. Second, the requirement for a dc-link bus of 14 V for an alternator unit that delivers almost 2.4 kW imposes the use of high phase current value resulting in significant stator voltage drops at the stator reactance (the ohmic part of the impedance can be neglected). As a result the necessity to overcome high stator voltage drops requires high back-emf values to be generated in order to supply the required load current. In addition, the need to keep the terminal voltage within limits imposes the introduction of a direct axis current, as opposed to control schemes where the direct axis current is set equal to zero [11].

The generation of the d-axis current results in the increase of the phase current and in turn of the stator copper losses and the rectifier losses. For this reason, the minimisation of this current component, which weakens the alternator's field, is of great importance. In order to achieve that, the phase current phasor must be close to the q-axis of the d-q plane. In this way the q-axis current is maximised and thus the alternator efficiency is increased. For this reason, a cost function that minimises the stator phase current through the minimisation of the alternator's losses is generated [12]. Only at very low power level can $I_d = 0$ [13].

IV. Control Algorithm

Stator copper losses of an automotive alternator are a big portion of the overall alternator losses [14]. The proposed control scheme is based on minimising these losses. The voltage limit of the alternator is given by the following equation:

$$\sqrt{V_d^2 + V_q^2} = \sqrt{2} * V_{LL} \tag{6}$$

where V_{LL} is the line-to-line terminal voltage. The later is related to the dc-link voltage usage allowed by the implemented modulation scheme. Substituting in (6) for steady-state conditions, equations (1) and (2), and taking into consideration that the stator's resistance voltage drop is much lower than that of the reactance:

$$I_d = \frac{\sqrt{2} M_f I_f \omega_r^e - \sqrt{(\sqrt{2} * V_{LL})^2 - (\omega_r^e L_s I_q)^2}}{\omega_r^e L_s} \tag{7}$$

Ignoring the losses at the rectification stage, the power balance between the alternator's electromagnetic generated power (P_{conv}) and the dc side of the converter, is:

$$P_{conv} = P_{cu}^s + P_{dc} \Rightarrow \frac{3}{2}\sqrt{2} M_f I_f \omega_r^e I_q = \frac{3}{2} R_s (I_d^2 + I_q^2) + P_{dc} \tag{8}$$

Iron losses are also ignored, as seen in equation (8), due to the lack of an analytic formula to predict them. Combining equations (7) and (8) and considering a given operation point: alternator speed of 2000 rpm, sPWM with a $14\ V$ dc bus voltage, modulation index of 0.925, and dc power level of 500 W, Fig.2 is generated. The point of maximum efficiency of the alternator occurs, Fig.2.b, where the phase current is minimised, Fig.2.a [12]. However, this does not mean d-axis or q-axis currents have minimum values as seen in Fig.2.a. In this way the reference values of the d-axis, q-axis and field current values are generated. This process is repeated for different speed points, power levels and modulation schemes in order to generate the optimum operating conditions where

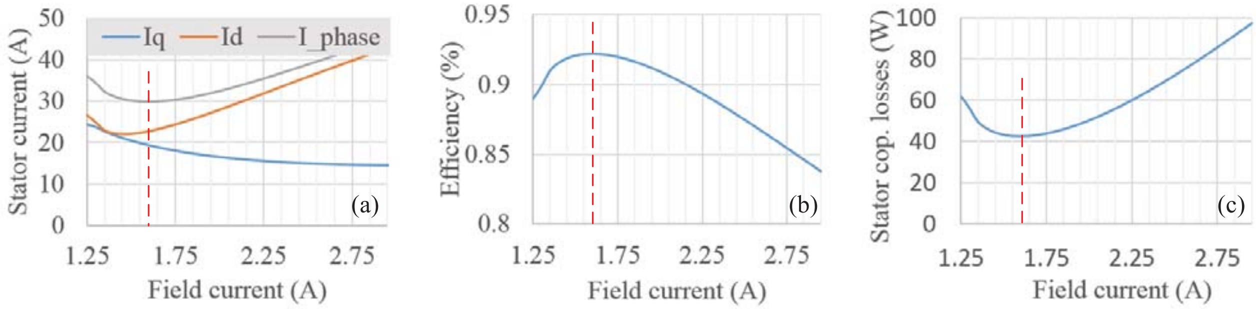

Fig. 2. a) Stator current values, b) Alternator efficiency c) Stator copper losses.

the alternator's efficiency is maximum. Fig.3 presents the operating points surface (in red) and the optimum operating points (in black). The surface shows as zero efficiency points the places where the power demand cannot be achieved for a given current. The maximum power level is defined by the thermal current of the alternator, which in turn is mainly limited by the alternator's phase current.

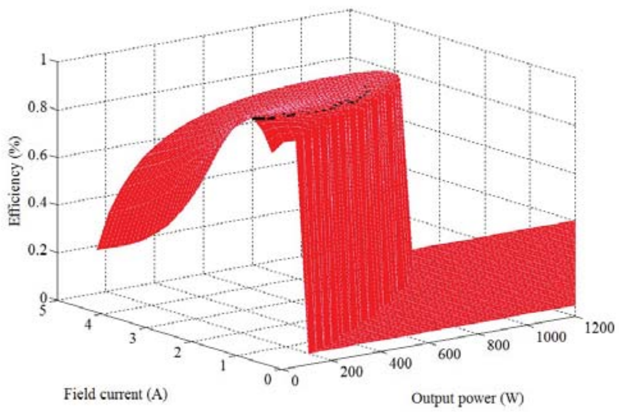

Fig. 3. Optimum efficiency operating points for 2000 rpm

V. Modulation Scheme Analysis

The proposed control strategy is implemented using three different modulation schemes, in order to evaluate the efficiency improvements they offer.

A. Sinusoidal PWM

sPWM uses a common high frequency triangular waveform to compare the three-phase sinusoidal waveforms for modulating and control [15]. To describe the rectifier in terms of a control state feedback block diagram the following equation is used [16].

$$\hat{V_{a1}} = 0.5 m_a V_{dc} \tag{9}$$

where m_a is the modulation amplitude ratio and is set to control the peak fundamental phase voltage $\hat{V_{a1}}$ with respect to the dc-link midpoint [16]. In this case a delta-connected alternator is used, thus the rms line-to-line voltage is given by:

$$V_{LL} = m_a \frac{\sqrt{3}}{\sqrt{2}} \hat{V_{a1}} \approx 0.612 m_a V_{dc} \tag{10}$$

B. Third Harmonic Injection

Third harmonic injection allows the reduction of the peak of the resultant modulating signal making better use of the dc-link voltage [15]. Therefore, the reference value of the generated modulating signals can be raised to values higher than those of the sPWM as seen in equation (9), leading to a higher alternator terminal voltage [15]. As a result, the maximum peak phase voltage of this scheme is equal to:

$$\hat{V_{a1}} = m_a \frac{0.5 V_{dc}}{sin(\frac{\pi}{3})} \approx 0.577 m_a V_{dc} \tag{11}$$

Transforming equation (11) into the rms line-to-line equivalent form as for the sPWM:

$$V_{LL} = m_a \frac{\sqrt{3}}{\sqrt{2}} \hat{V_{a1}} \approx 0.707 m_a V_{dc} \tag{12}$$

Comparing equation (11) to the voltage obtained from sPWM scheme in equation (9) for the same m_a, there is an increase of 15% [15]. The implementation of this scheme uses the "MIN-MAX" technique according to [17], which produces the same results as of the direct injection of one sixth of the third harmonic component to the control voltages. This implementation is in essence equivalent to symmetrical SVM in terms of harmonic distortion [18].

C. Space Vector Modulation

SVM technique allows to represent the rectifier's input voltages to space phasors [15]. This paper uses a discontinuous version of SVM, where switching is not continuous. Therefore one leg of the rectifier does not switch during the switching cycle and is tied either to the negative or the positive dc-link bus voltage [15]. In this way the number of commutations are reduced to two thirds of the continuous SVM, reducing switching losses [15]. Finally, the voltage usage of any SVM technique, continuous or discontinuous, is the same as that of the third harmonic injection scheme [15], [18].

D. Comparison of Modulation Schemes

Table I presents the number of commutations per switching period and the dc-link voltage usage of every modulation scheme deployed in the content of this paper.

TABLE I. Commutations number per switching cycle and use of dc-link voltage of the implemented modulation schemes

Modulation Scheme	Commutations	V_{LL} (Vrms)
sPWM	12	0.612 V_{dc}
3rd Harmonic	12	0.707V_{dc}
DSVM	8	0.707V_{dc}

The ratio between the modulated frequency and the trigger frequency defines the frequency modulation ratio as [16]:

$$m_f = \frac{f_s}{f_{trigger}} \tag{13}$$

The above ratio should be an odd integer multiple of three [16]. First, if m_f is not an integer the PWM becomes asynchronous and sub-harmonics of the fundamental might be generated [15]. Second, the value of m_f should be an odd integer multiple of three in order to cancel the triplen harmonics from the harmonic currents generated by the rectifier [15], [16]. However, while the alternator speed increases the generated voltage frequency steps up, changing m_f. The latter could be adjusted according to the generated operating frequencies using usually a hysteresis block [15], but that leads to changing the switching frequency of the rectifier, so consistent measurement of the rectifier losses throughout the different speed points would not be possible. For this reason, a number of different speed points were selected representing idle to cruising speed, with a frequency modulation ratio, which is an odd integer multiple of three in all cases as seen in Table II.

TABLE II. Experimental speed points

ω_r (rpm)	$f_{fundamental}$ (Hz)	f_{sw} (kHz)	m_f
2000	266.67	20	75
3846	512.82	20	39
5555	740.73	20	27

VI. Simulation of the System

The control scheme, presented in Fig.4, is implemented both in simulation and experiment.

Cascaded PI controllers are used to control the d-axis and q-axis currents as well as the field winding current. Initially, the PI controllers are designed by linear analysis of the investigated system's plant (stator/rotor circuit and active-rectifier) in Simulink and selecting an appropriate frequency response for every PI controller according to their Bode diagrams. Simulink's "Linear Analysis Tool" is used for the plant analysis, while Matlab's "sisotool" is used for tuning the respective PI controllers. The inner dq-axes current loops are closed at 2 kHz, while the dc-bus voltage at 200 Hz. The field

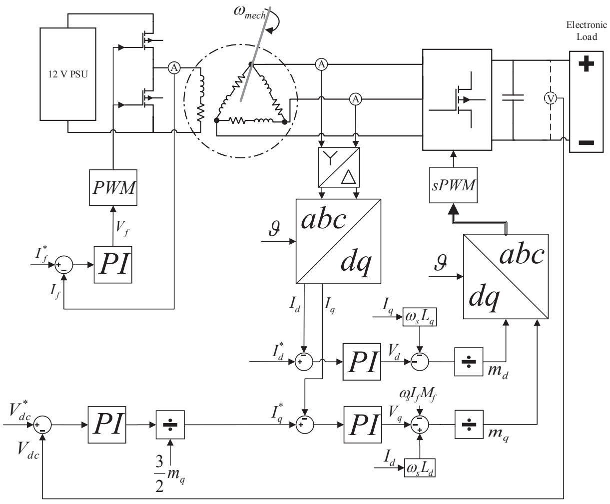

Fig. 4. Control scheme schematic of the alternator/active rectifier system

controller is selected at 10 Hz. The d-axis and field current references are introduced using look-up tables according to the speed of the alternator and the q-axis reference generated by the dc-link voltage controller.

The switching frequency of the rectifier is set at 20 kHz, which is above audible noise, and is kept at this value throughout the different speed points.

VII. Experimental Set-up

A three-phase bridge rectifier, depicted in Fig.5, using Infineon IPP120N08S4-03 OptiMos semiconductor devices was designed and built.

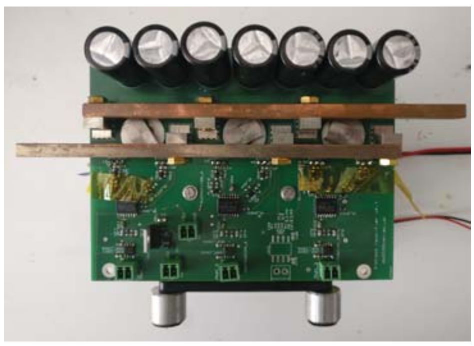

Fig. 5. Active rectifier topology

A dc chopper together with voltage and current sensors for the experimental implementation were also designed and built. The position is sensed by a quadrature incremental encoder with 2000 ppr. DC voltage, two ac line currents and position are fed to a TI DSP control card. VisSim software is used to implement the control strategy designed in Matlab/Simulink. The software allows not only the control of the system but also condition monitoring of the sensed values during the rectifier's operation. The efficiency measurements are carried out with

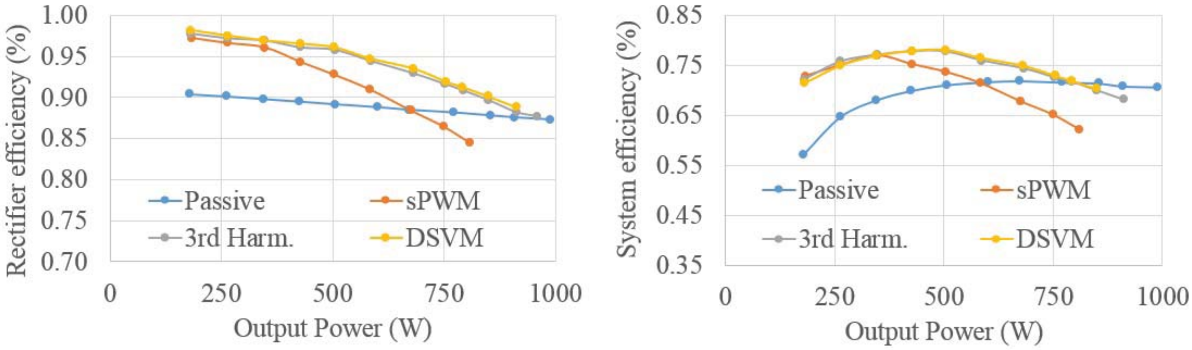

Fig. 6. Rectifier and system efficiency measurements for 2000 rpm

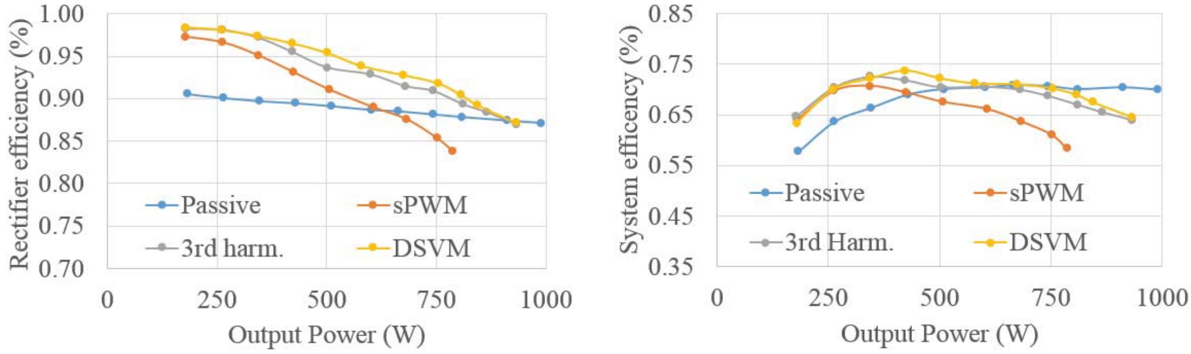

Fig. 7. Rectifier and system efficiency measurements for 3846 rpm

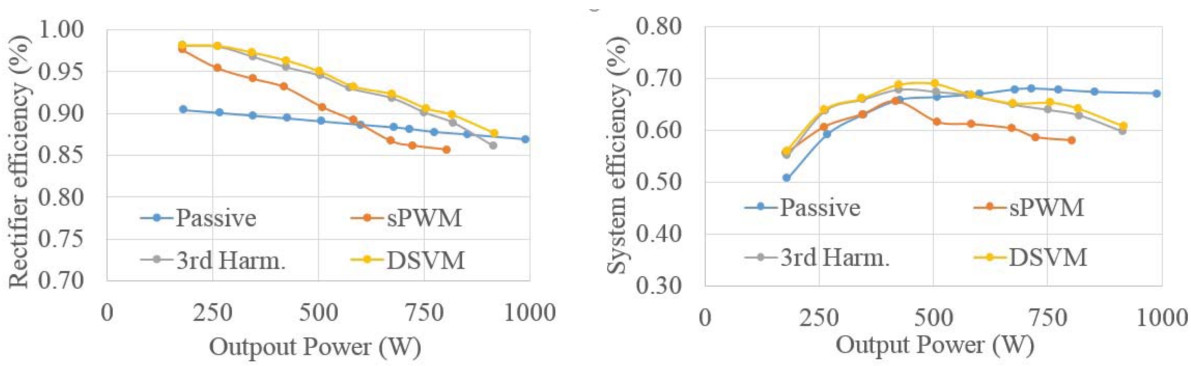

Fig. 8. Rectifier and system efficiency measurements for 5555 rpm

two N4th PPA5530 power analysers and calibrated current shunts. Fig.9 presents the alternator's test-rig. A conventional vehicle's Internal Combustion Engine (ICE) crankshaft speed varies typically between 800 rpm and 3000 rpm for idle and cruising speed, respectively. The crankshaft pulley to alternator pulley ratio is around 2.5, thus the alternator's speed range is between 2000 rpm and 7500 rpm. Taking into consideration the above, a test bench was designed and configured, capable of simulating the ICE operation and the existing drive-belt gear ratio.

VIII. Results Discussion

The steady-state measurements of the proposed control strategy using different modulation schemes resulted in the efficiency curves presented in Fig.6 to Fig.8. The body diodes of the rectifier are used for passive rectification in an effort to use comparable components. Three power measurements were captured during the tests conduction, the input mechanical power to the alternator (P_{mech}), the ac generated power (P_{ac}) and the power at the dc side of the system (P_{dc}). The rectifier efficiency (P_{dc}/P_{ac}) is presented on the left of every figure, while the overall system's efficiency (P_{dc}/P_{mech}) is depicted on the right.

DSVM and 3rd harmonic injection utilise approximately

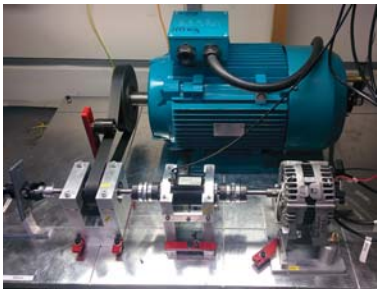

Fig. 9. Alternator test-rig

15% more dc-link voltage, thus the calculated current values are lower than those of the sPWM [15]. Therefore, higher overall, system and rectification efficiency is achieved compared to sPWM. DSVM features fewer commutations (8) per cycle than 3rd harmonic injection, as a result there are lower switching losses, thereby reducing rectifier losses [15]. However, the lower number of commutations results in a more distorted ac current waveform, increasing in this way the alternator iron losses [15]. The rectifier and the system efficiency of the active-rectifier's modulation schemes is compromised, while increasing the speed of the alternator, resulting in crossing the passive rectifier's efficiency curve at an earlier point. This behaviour is due to the increase of the stator reactance with speed, resulting in lower I_q/I_d ratios as the speed increases and consequently stator current and losses increase. The overall system's efficiency of the active-rectifier seems to be compromised with the speed increase too. This could be associated to the generated harmonics on the ac side values as well as the high inductance value of the alternator that requires high d-axis current values.

IX. Conclusions and Future Work

A control design for a Lundell alternator is discussed and implemented using a test-rig. Three different modulation schemes are presented to quantify the efficiency improvements that could introduce, both for the alternator and the overall system. The results of the proposed control strategy are compared against passive rectification. The scheme allows the minimisation of the stator copper losses and the implementation of the DSVM permitting to reduce the switching losses while increasing the overall system efficiency. It is evident that the modulation technique plays a significant role in the system efficiency for automotive Lundell alternators used in such applications. However, the system's efficiency at higher speed and power levels is compromised compared to the passive rectification. Therefore, an active-rectifier can be used at low speed levels, where the alternator can only deliver a portion of its output power, while the passive rectifier can be used for higher speed and power levels ($\geq$3846 rpm) generating in this way a hybrid control scheme for the overall alternator operation range.

The authors intent to extend this work by introducing a symmetrical version of SVM with only 6 commutations per switching cycle in an effort to reduce switching losses further. In addition, the harmonic analysis of the generated ac values of the different modulation schemes will be performed in order to quantify any relations between the modulation scheme and the harmonic distortion on the ac side. Finally, energy losses estimation from a double pulse test will allow to better understand the switching losses of the active-rectifier.

References

[1] *Automotive electrics, automotive electronics*, 5th ed. Plochingen: Robert Bosch GmbH ; Wiley, 2007.

[2] S. Rees and U. Ammann, "A smart synchronous rectifier for 12 v automobile alternators," in *Power Electronics Specialist Conference, 2003. PESC '03. 2003 IEEE 34th Annual*, vol. 4, June 2003, pp. 1516–1521 vol.4.

[3] T. O'Gorman, D. Stephens, T. Bohn, and R. Carlson, "Automotive alternator synchronous rectificaton via self-sensing method for improved vehicle fuel consumption," in *Industry Applications Conference, 2007. 42nd IAS Annual Meeting. Conference Record of the 2007 IEEE*, Sept 2007, pp. 1726–1730.

[4] T. O'Gorman, D. Stephens, B. Conway, and T. Bohn, "A rotor and stator method to increase the power available from an automotive alternator at idle speed," in *Applied Power Electronics Conference and Exposition, 2008. APEC 2008. Twenty-Third Annual IEEE*, Feb 2008, pp. 1991–1998.

[5] F. Liang, J. Miller, and S. Zarei, "A control scheme to maximize output power of a synchronous alternator in a vehicle electrical power generation system," in *Industry Applications Conference, 1996. Thirty-First IAS Annual Meeting, IAS '96., Conference Record of the 1996 IEEE*, vol. 2, Oct 1996, pp. 830–835 vol.2.

[6] F. Liang, J. M. Miller, and X. Xu, "A vehicle electric power generation system with improved output power and efficiency," *IEEE Transactions on Industry Applications*, vol. 35, no. 6, pp. 1341–1346, Nov 1999.

[7] R. Ivankovic, J. Cros, and P. Viarouge, "Experimental comparison of rectifiers for lundell automotive alternators," in *Power Electronics and Applications, 2009. EPE '09. 13th European Conference on*, Sept 2009, pp. 1–10.

[8] R. De Doncker, D. Pulle W.J., and A. Veltman, *Advanced electrical drives : analysis, modeling, control*. Dordrecht: Springer, 2011.

[9] B. Bose, *MODERN POWER ELECTRONICS AND AC DRIVES*, 3rd ed. Prentice Hall, 2002.

[10] D. J. Perreault and V. Caliskan, "Automotive power generation and control," *IEEE Transactions on Power Electronics*, vol. 19, no. 3, pp. 618–630, May 2004.

[11] M. Alnajjar and D. Gerling, "Minimization of energy losses in the traction drive of hev using optimized adaptive control," in *2014 IEEE Vehicle Power and Propulsion Conference (VPPC)*, Oct 2014, pp. 1–6.

[12] Z. Xu, D. Zhang, F. Wang, and D. Boroyevich, "A unified control for the combined permanent magnet generator and active rectifier system," *IEEE Trans. Power Electron.*, vol. 29, no. 10, p. 5644ÃćâĆňâĂIJ5656, Oct 2014. [Online]. Available: http://dx.doi.org/10.1109/TPEL.2014.2300191

[13] I. Boldea, G. D. Andreescu, C. Rossi, A. Pilati, and D. Casadei, "Active flux based motion-sensorless vector control of dc-excited synchronous machines," in *2009 IEEE Energy Conversion Congress and Exposition*, Sept 2009, pp. 2496–2503.

[14] S. C. Tang, T. A. Keim, and D. J. Perreault, "Thermal modeling of lundell alternators," *IEEE Transactions on Energy Conversion*, vol. 20, no. 1, pp. 25–36, March 2005.

[15] H. Abu-Rub, *High performance control of AC drives with MATLAB*, 9781119942108th ed. Chichester, West Sussex ; Hoboken, NJ: Wiley, 2012. [Online]. Available: http://ezproxy.lib.cam.ac.uk:2048/login?url=http://onlinelibrary.wiley.com/book/10.1002/9781119969242

[16] N. Mohan, *Power electronics : converters, applications, and design*, 3rd ed. Hoboken, N.J. ; [Chichester]: Wiley, 2003.

[17] Microsemi. (2014) Space vector pulse width modulation mss software implementation, user guide. [Online]. Available: http://www.microsemi.com/document-portal/cat_view/56661-internal-documents/56758-soc/56785-guides?dir=ASC&lang=en&limit=20&limitstart=220&order=name

[18] D. G. Holmes, *Pulse width modulation for power converters : principles and practice*. Piscataway, N.J: IEEE Press ; Wiley, 2003.